



Effective high-order harmonic generation from metal sulfide quantum dots

RASHID A. GANEEV,^{1,2} GANJABOY S. BOLTAEV,¹ VYACHESLAV V. KIM,¹
KE ZHANG,¹ ANDREY I. ZVYAGIN,² MICHAEL S. SMIRNOV,² OLEG V.
OVCHINNIKOV,² PAVEL V. REDKIN,¹ MICHAEL WÖSTMANN,³ HELMUT
ZACHARIAS,³ AND CHUNLEI GUO^{1,4,*}

¹The Guo China-U.S. Photonics Laboratory, State Key Laboratory of Applied Optics, Changchun Institute of Optics, Fine Mechanics and Physics, Chinese Academy of Sciences, Changchun 130033, China

²Faculty of Physics, Voronezh State University, 1 University Square, Voronezh 394018, Russia

³Center for Nanotechnology, Westfälische Wilhelms-Universität 48149 Münster, Germany

⁴The Institute of Optics, University of Rochester, Rochester, NY 14627, USA

*guo@optics.rochester.edu

Abstract: In the past, common media for high-order harmonic generation (HHG) has been atoms and molecules. More recently, clusters, and nanoparticles have been introduced as HHG emitting media. Multi-particle media can enhance HHG yields but have more stringent requirements in determining the optimal parameters. Here, we demonstrate, for the first time, the effective application of 1-3 nm metal sulfide quantum dots (QDs) for harmonic generation in the 20 – 115 nm extreme ultraviolet range. We report on the syntheses, ablation of Ag₂S, CdS, and ZnS QDs, and HHG from laser-produced plasmas by using single- and two-color pumps. We compare HHG efficiency from the ablated QDs to that of bulk metal sulfides and show a seven-fold increase in harmonic yields. Further, the study also allows us to understand the effects of QD-contained plasma spreading dynamics on HHG yield.

© 2018 Optical Society of America under the terms of the [OSA Open Access Publishing Agreement](#)

1. Introduction

Laser ablation has been studied extensively in material applications [1]. Laser ablation can readily produce plasmas containing neutrals and ions, as well as clusters, quantum dots (QDs) and nanoparticles that could be used for different applications. One application for the ablated media is that it can be used as emitters for harmonic generation from ultrashort laser pulses. The practical aspects of these studies include formation conditions for efficient emission of coherent extreme ultraviolet (XUV) radiation through high-order harmonic generation (HHG) with further applications in different fields of physics, chemistry, and biology. The enhanced harmonic generation has been demonstrated using clusters and nanoparticles in the cases of gas HHG [2–10] and plasma HHG [11–13].

Previous studies on HHG after ablation of nanoparticle-containing targets have revealed the advantages of such species for frequency conversion in the XUV range. A larger cross-section of recombination and the possibility of recombination of an accelerated electron with the parent particle through either recombination with the same or a neighboring atom, or with the multi-atomic particle as a whole, were considered as the most probable reasons for the growth of HHG yield in such plasmas. In these earlier studies, the experimental conditions were not optimized, in particular, the delay between the heating and driving pulses. Nevertheless, even at those non-optimal conditions, the harmonic yield was already higher than in the case of ablation of bulk targets of the same material [14]. Since in these studies short delays of up to 100 ns between the heating and driving pulses were employed, it was not clear how nanoparticle species could influence the processes of frequency conversion, because there were no proofs of their presence in the interaction region with the driving laser.

One explanation was based on the disintegration of larger species into small clusters and monoatomic species, which probably could reach the interaction area at the short delays employed. However, no sufficient confirmation of this assumption has been provided. Taking into account the anticipated velocities of atoms, molecules and ions ($\sim 1 \times 10^4 \text{ m s}^{-1}$), QDs ($\sim 1 \times 10^3 \text{ m s}^{-1}$) and nanoparticles [$(1-5) \times 10^1 \text{ m s}^{-1}$] of the same material [15] one can expect their arrival in the region of the femtosecond laser beam propagation a few tens of nanosecond, a few hundreds of nanosecond, and a few tens of microsecond from the beginning of ablation, respectively.

To match the propagation of the driving pulse and the highest concentration of the studied group of multi-atomic species one, therefore, has to use the electronic delay between the heating and the driving pulses. The application of two electronically separated pulses from different lasers synchronized by a digital delay generator allows analyzing the involvement of various species in such multi-particle plasmas in the HHG process. This method has earlier been used in the case of third harmonic generation in a laser plasma [16,17]. Application of this approach for HHG in multi-particle plasmas, alongside with other methods of harmonic enhancement, requires the analysis of the ablated species to temporally match them with the propagation of driving femtosecond pulses through the plasma.

The QD-containing materials, particularly metal sulfide based QDs, have attracted special attention due to their large low-order optical nonlinearities [18,19]. Particularly, various nonlinear optical processes can be induced in the ZnS nanoparticles, which became useful in photonics [20–22]. The coexistence of reverse saturable absorption and two-photon absorption in silver sulfide suggests that Ag_2S QDs could be a very promising nonlinear medium for photonic devices in different time scales if these semiconductor nanocrystallites are incorporated into appropriate media while retaining the attractive features of both components. The Ag_2S QDs also demonstrate low-threshold optical limiting in the visible and near-IR ranges [23–25]. To the best of our knowledge, there are so far no studies devoted to the analysis of the high-order nonlinear optical properties of metal sulfide QDs.

A search for new applications of QDs is an important task for the optical community. The interesting idea is to find the optimal conditions in the application of such QDs as effective emitters of the high-order harmonics of femtosecond pulses for the development of efficient sources of coherent XUV radiation. In this paper, we demonstrate for the first time HHG in such QDs using electronically driven delays between the heating and driving lasers. We ablate Ag_2S , CdS and ZnS QDs using a nanosecond laser and demonstrate efficient HHG in plasmas using a femtosecond laser. With this approach, we achieved effective harmonics generation in the spectral range from 20 to 115 nm using such QDs.

2. Experimental arrangements

2.1 Preparation of QD-containing targets

Improving the efficiency of HHG in a plasma containing QDs requires solving two problems: (1) developing the methods for the synthesis of metal sulfides QDs, followed by the formation of solid-state materials containing large concentrations of these species, and ensuring the stability of the morphology of vaporized materials under laser ablation, and (2) optimizing the process of converting the wavelength of laser pulses during the HHG in a laser plasma containing such multi-particles.

The synthesis of QDs was carried out taking into account a number of criteria for their use to generate harmonics of ultrashort pulses. The first criterion is the formation (as a result of ablation of samples by either picosecond or nanosecond heating pulses) of a plasma cloud consisting of QDs, as well as atoms, ions, and clusters at the time of the passage of the converting femtosecond pulses above the target surface. The second criterion is the presence of the maximal concentration of QDs at the time of transmission of the femtosecond pulses through the plasma. The third criterion is the size characteristics of quantum dots. Previous

studies of harmonic generation in multi-particle containing plasmas, as well as qualitative assessments, show that the most optimal sizes of such species should be in the range of 1 - 4 nm (see also the discussion section).

Synthesis of colloidal QDs of ZnS and CdS was carried out by mixing the $\text{CdBr}_2 \times 4\text{H}_2\text{O}$, $\text{ZnBr}_2 \times 4\text{H}_2\text{O}$ and thioglucolic acid (TGA) in the required proportions. The corresponding salts of cadmium and zinc bromide were dissolved in water (200 ml) and then the TGA was added. Then the 50 ml of Na_2S aqueous solution (1.3 mM) was injected into the prepared solution. The synthesized colloidal solution of QDs was dissolved by adding ethanol to a 50% solution, centrifuged and re-dissolved in water. The cleaning procedure was repeated several times. A similar procedure was used for the synthesis of Ag_2S QDs.

The synthesized samples of colloidal solutions of zinc, cadmium and silver sulfides were further used to produce the solid targets for laser ablation and generation of harmonics. We developed a new method of increasing the filling factor Ag_2S , ZnS and CdS QDs in the stabilizing polymer to form solid samples of multi-particle species for laser ablation in vacuum and formation of the plasma torches containing a large amount of QDs required for efficient generation of harmonics. The method is based on the compatibility of synthesized colloidal QDs and gelatin, as well as the possibility of increasing the concentration of QDs during centrifugation in the presence of acetone. Gelatin's property of high filling ability as a polymer and the possibility of drying such samples to a solid state are among the advantages of this method. The preparation of solid tablets was accomplished in the following sequence: the prepared concentrated solution of QDs was introduced into the gelatin melted at a temperature of 40-50 °C using intensive stirring and then the suspensions were dried at a temperature of 80 °C for 24 hours to a solid state and then placed for further vacuum drying where they were kept for 10 days. Control of the obtained samples was carried out by analysis of their luminescence, which was compared with the luminescence of the same QDs in TGA. We observed a weak difference in the spectra of these two cases.

2.2 Plasma HHG setup

Synchronization of two laser sources, such as most commonly used Ti: sapphire femtosecond laser and Nd: YAG nanosecond laser, may resolve, to some extent, the puzzle related with the observation of the enhancement of the harmonics generating in the plasmas produced during ablation of multi-particle media. The main advantage of this approach is a possibility to electronically drive the delay between heating nanosecond and driving femtosecond pulses in a broad range. Additionally, the use of radiation from the nanosecond Nd: YAG lasers offers advantages in plasma formation compared with previously used picosecond pulses. The application of nanosecond pulses to ablate the targets allows the formation of less ionized and less excited plasma during a longer period of laser-matter interaction compared with the picosecond pulses. Nd: YAG lasers commonly operate at 10 Hz pulse repetition rate, which is more suitable for stable HHG in plasmas compared with 1 kHz ablation, though in the latter case some strategies, such as target rotation [26], allowed, to some extent, improvement of the stability of 1 kHz coherent short-wavelength sources.

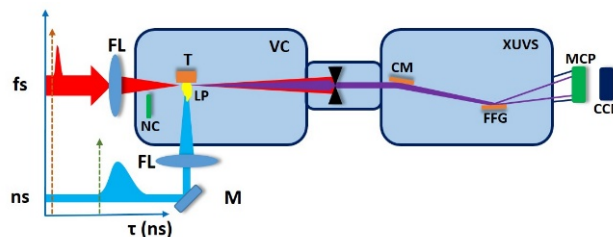


Fig. 1. High-order harmonic generation setup. fs, converting femtosecond pulses, ns, heating nanosecond pulses; FL, focusing lenses; VC, vacuum chamber; T, target; NC, BBO crystal;

LP, laser plasma; XUVS, extreme ultraviolet spectrometer; CM, cylindrical gold-coated mirror; FFG, flat field grating; MCP, microchannel plate; CCD, CCD camera.

The metal sulfide QD plasmas were used for HHG. The driving femtosecond pulses (800nm, 1 kHz; Spitfire Ace, Spectra Physics) propagated through the plasma at different delays from the beginning of target irradiation by nanosecond heating pulses (1064 nm, 10 Hz; Q-Smart, Coherent). The variable delay ($0 - 10^6$ ns) between 5 ns heating pulses and 30 fs driving pulses was established to generate harmonics in plasma at the used geometry of experiments when the 800 nm femtosecond pulses were focused onto the plasma area from the orthogonal direction with regard to ablating radiation, at a distance of $\sim 200 \mu\text{m}$ above the target surface (Fig. 1). Additionally, the harmonic yield was maximized by adjusting the position of the target with regard to the optical axis of propagation of the driving femtosecond pulses and by varying the focusing position of this radiation with regard to the plasma. The harmonic emission was directed to the XUV spectrometer containing a cylindrical mirror and a 1200 grooves/mm flat field grating with variable line spacing. The XUV spectrum was recorded by a micro-channel plate (MCP) with a phosphor screen, and the harmonics were imaged by a CCD camera.

We also carried out the HHG using the two-color pump (TCP) of plasma. The reason for using the TCP instead of the single-color pump (SCP) was related with earlier demonstrated advantages of this approach in the generation of odd and even harmonics in gases and plasmas [27–31], as well as larger efficiency of harmonic yield in the former case. The TCP using 800 nm radiation as the first field and 400 nm radiation as the second field was applied to carry out the comparative analysis of TCP and SCP schemes. The 0.4-mm-thick BBO crystal (type I) was installed inside the vacuum chamber on the path of the 800 nm radiation to generate second harmonic (H2). The conversion efficiency of H2 pulses ($\lambda = 400$ nm) was relatively low ($\sim 4\%$). However, due to small group velocity dispersion in the thin BBO crystal, the overlap of these two pulses in plasma area was sufficient to determine how the weak second orthogonally polarized field influences the whole process of HHG in QDs.

3. Results

3.1 Characterization of QDs

The originality of the general approach to increase the HHG efficiency is based on the choice of quantum confined multi-atomic particles to facilitate an increase of the nonlinear optical response of the plasma medium. Qualitatively, an increase of the cross section for the recombination of accelerated electrons with the multi-particle species with increasing size of the parent particle can be expected. However, this assumption is valid only up to certain sizes of multi-particle species. A further increase of the number of atoms or molecules in the particle leads to conditions where the atoms or molecules located inside the particle become completely shielded and thus eliminated from the three-step process of HHG, i.e., ionization, acceleration, and recombination. In other words, the internal atoms and molecules do not supply electrons for acceleration and recombination. Thus, the optimal size of the particles is one of the most important characteristics in order to achieve an increase in the efficiency of harmonic generation. Moreover, its importance rises with increasing order of the generated harmonic. Early studies carried out in gases and plasmas have shown an increase of HHG intensity using clusters containing up to 1000 noble gas atoms, as well as using nanoparticles containing tens of thousands to a few millions of atoms. It turned out that the optimal number of atoms in the particles seems to lie in an intermediate size region. If one divides the aggregates into three categories like clusters (0.1 - 1 nm), QDs (1 - 6 nm), and nanoparticles (10 - 100 nm), then the second group seems to be the most promising for HHG. The QDs synthesized in this work are satisfying this criterion.

Samples of colloidal QDs were characterized by x-ray diffraction, transmission electron microscopy (TEM), optical absorption, and luminescence spectroscopy. The composition of

the particles was determined by x-ray and electron diffraction. The dispersion of the particle sizes was determined by statistical data analysis of the TEM images of the QDs. TEM also provided information on the morphology of the QDs. The analysis of the structure, phase composition, and morphology of the samples allowed improvements to the synthesis techniques.

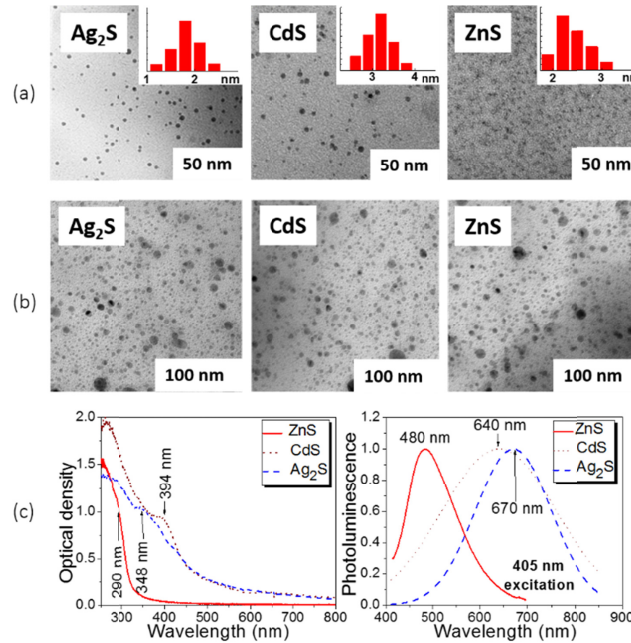


Fig. 2. (a) TEM images of synthesized metal sulfide QDs. (b) TEM images of the Ag₂S, CdS and ZnS QDs ablated at the 10 mJ energy of heating nanosecond pulse and deposited on nearby glass and silicon substrates. (c) Spectra of (left graph) optical absorption and (right graph) photoluminescence of synthesized QD.

The TEM images of synthesized metal sulfide QDs are shown in Fig. 2(a). The size distribution is shown in the inset as histograms. From the histograms, we conclude that Ag₂S QDs show mean sizes in the range of 1.7 to 2.0 nm, CdS QDs about 3.0 to 3.2 nm, and ZnS QDs about 2 to 2.2 nm diameter. The morphological studies reveal that Ag₂S QDs condensate in a monoclinic lattice, while CdS and ZnS QDs condensate in a cubic lattice and Ag₂S QDs in a monoclinic lattice. Figure 2(b) presents images of the QDs ablated by 10 mJ and 5 ns pulses and deposited on nearby substrates. The collected particles confirm the presence of metal sulfide QDs within the plasma plume. The sizes of deposited particles were larger than those of original ones. Optical absorption and photoluminescence spectra are shown in Fig. 2(c). The spectra were significantly blue shifted with regard to the bulk materials of similar materials. The CdS, ZnS and Ag₂S QDs were embedded in gelatin with about 20% weight and prepared in the form of 5 × 5 × 3 mm plates.

3.2 Harmonic generation

Figure 3 shows high-order harmonics generated from these QDs in the spectral range of 20 – 120 nm. HHG at different delays between the heating and driving pulses from 100 to 2000 ns is shown for pulse energies of 4 and 0.4 mJ, respectively. At initial stages of plasma formation and spreading out from the target, i.e., at delays less than 50 ns, the concentration of particles (neutrals and singly charged ions) was insufficient for HHG, since the whole ensemble of particles possessing velocities of $\sim 2 \times 10^4$ m s⁻¹ cannot reach the spatial region of the driving beam. At larger delays (above 100 ns) sufficient amounts of QDs appeared in

the path of the femtosecond beam which allowed the generation of harmonics. The optimal delay was different for three QD plasmas studied. At about 400, 300, and 250 ns the highest harmonic yield was observed for Ag₂S QD (atomic weight 247.8 amu), CdS QD (144.5 amu), and ZnS QD (97.5 amu), respectively. Notice that the use of a carbon plasma (atomic weight 12 amu) yielded maximal harmonic intensity at a significantly smaller delay of 30 ns between the heating and driving pulses using similar pulse energies. It should also be mentioned that harmonics generated from pure gelatin were almost one order of magnitude lower than those observed from the QDs. The harmonic cut-off is higher for lighter QD species, e.g., at the 31st harmonic for ZnS while Ag₂S showed the 25th as highest harmonic. A further increase of the delay for each of these plasmas led to a gradual decrease of the HHG efficiency. The harmonics almost disappeared once the delay exceeded 2 to 3 μ s. No harmonics were observed at delays up to 50 μ s.

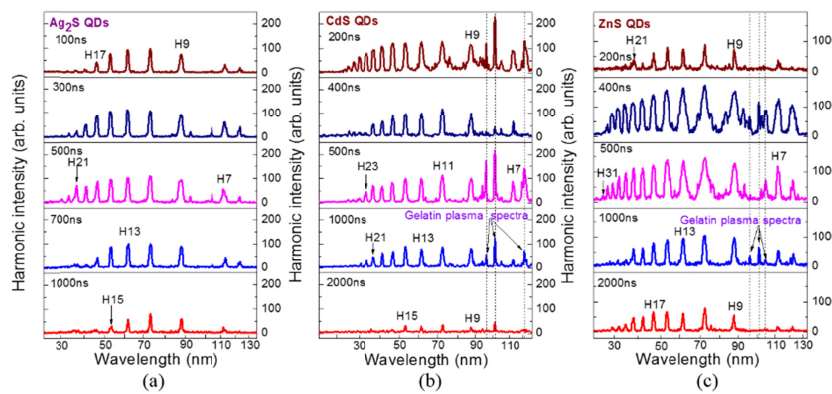


Fig. 3. Harmonic spectra from QD-containing plasmas [(a) silver sulfide QDs, (b) cadmium sulfide QDs, (c) zinc sulfide QDs] at different delays between heating and driving pulses. Dash-dotted lines show the plasma elision attributed to overexcited gelatin.

Experiments using bulk targets of the same materials led to similar dependencies of the harmonic yield on the delay between the heating and driving pulses. These experiments showed that independently of whether molecules or QDs spread out from the target surface of the same material they appear in the area of the femtosecond beam approximately at the same time. Figure 4(a) shows the harmonic generation in the laser-produced plasma after ablation of bulk ZnS by 4 mJ pulses. The harmonic yield maximizes at about 200 – 500 ns delay.

Figure 4(b) shows a comparison of the harmonic yield in the case of ablation of bulk and QD-containing ZnS targets. It is obvious that the QD plasma yield significantly stronger harmonics which also extend to higher orders. In the case of QD-containing plasma, the harmonics extended to \sim 50 eV (25 nm) or 31st order, while for the plasma produced from bulk ZnS the highest generated harmonic order was the 16th corresponding to a photon energy of \sim 26 eV (47 nm). The weight concentration of ZnS QDs in gelatin (0.2) was taken into account to carry out the comparison of the HHG spectra produced from monoparticles and multi-particle plasma. The overall ratio of intensities of the lower-order harmonics generated in these two plasmas was \sim 7.

Figure 5 shows the plasma emission spectra of Ag₂S, CdS and ZnS QDs in gelatin (three upper panels) and pure gelatin (bottom panel) using a larger energy of heating pulses (15 mJ). The majority of lines belong to gelatin emission, except the shorter-wavelength part of this spectrum. Most of the lines can be assigned to the emission from ionized carbon, as expected for gelatin. Those in the range of 45 – 90 nm seem mostly related with the C II emission. Probably, the existence of singly charged carbon caused the harmonic generation in pure gelatin plasma. These spectra underline that the metal sulfides were weakly excited and

ionized during ablation. This condition of “mild” ablation, when the existing density of free electrons in the plasma do not prevent the formation of phase matching conditions between the waves of the driving and harmonic fields, is a prerequisite for efficient HHG. Notice that the conditions of ablation, when the plasma emission shown in Fig. 5 dominates in the XUV spectra, are unsuitable for efficient HHG due to the presence of a large number of free electrons which prevent an optimal phase relation between the driving and harmonic waves.

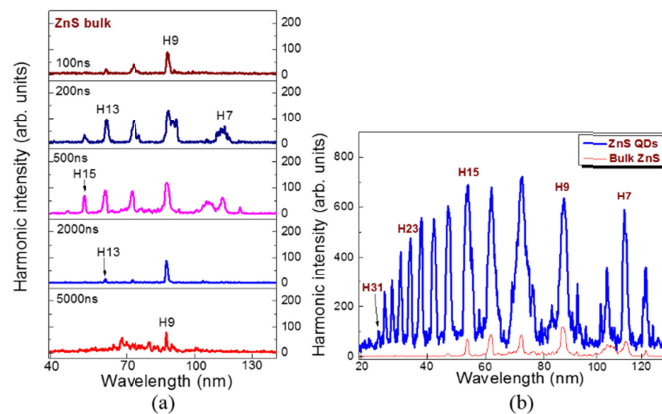


Fig. 4. (a) Harmonic spectra from the plasmas produced on the bulk ZnS surface at different delays between heating and driving pulses. The bottom panel was obtained at stronger excitation of the target (10 mJ). One can see the plasma emission lines from bulk zinc sulfide. (b) Comparison of harmonic distribution and intensities in the case of ablation of the QD (thick curve) and bulk (thin curve) ZnS targets at 500 ns delay between the heating and driving pulses. The weight part of QDs in gelatin (20%) is taken in to account for comparison of HHG at similar concentrations of plasmas.

Less excitation of the QD containing targets (4 mJ) allowed the formation of plasmas suitable for harmonic generation. Odd harmonics of 800 nm radiation up to H25, H29 and H31 were achieved using Ag₂S, CdS, and ZnS QD plasmas, respectively (see Fig. 3). The appearance of strong harmonic emission did not coincide with the plasma emission from highly charged particles in the studied spectral range (20–120 nm), which confirms that these experiments were carried out at a soft ablation regime of QD containing targets. The driving pulse [$I \approx (2-5) \times 10^{14} \text{ W cm}^{-2}$] also did not cause the appearance of strong ionic emission from higher charged molecules and QDs.

A final set of HHG studies was performed using two orthogonally polarized driving pulses. A 0.4 mm thick BBO crystal inserted inside the vacuum chamber on the path of the 800 nm fundamental radiation allowed the generation of 400 nm pulses while maintaining sufficient temporal and spatial overlap of 800 and 400 nm fields in the preformed plasmas. Notice that even only a small conversion efficiency (~5%) into the 400 nm radiation allowed the generation of the lower-order even harmonics alongside with the odd ones (Fig. 6, dash-dotted curves). We observed even harmonics generation up to H14. The seemingly relatively small yield of low-order harmonics (H6 to H9) was caused by a weaker sensitivity of the MCP detector for wavelengths above 100 nm.

The conversion efficiency of even harmonics in the case of TCP was higher than of odd harmonics in the case of SCP, despite a very low pulse energy of the 400 nm radiation with respect to the 800 nm one (~1:20). As it was underlined by Kim *et al.* [32] that in the case of two-color pumping stronger harmonics generation is possible due to the formation of a quasi-linear field, the selection of the short quantum path component which has a denser electron wave packet, and a higher ionization rate compared to SCP. The orthogonally polarized second field also participates in the modification of the trajectory of the accelerated electrons

from being two-dimensional to three-dimensional, which may lead to a removal of the medium symmetry. With suitable control of the relative phase between the fundamental and the second harmonic radiation, the latter field enhances the short path contribution, resulting in a clean spectrum of harmonics. One can see that even at a very small ratio of 400 and 800 nm pulse energies the influence of the weak field was sufficient to strongly modify the whole harmonic spectrum compared to the single color pumping case.

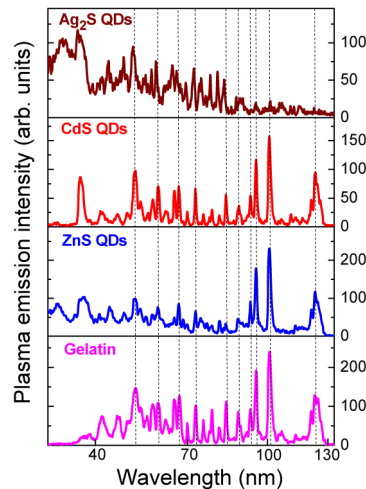


Fig. 5. Plasma emission spectra of Ag₂S, CdS and ZnS QDs in gelatin (three upper panels) and pure gelatin (bottom panel). Dash-dotted lines show similar emission in all four plasmas.

Notice the relative weaker H12 compared to H10 and H14. This heterogeneity in the even harmonic yields was caused by group velocity dispersion in the 0.4mm thick BBO crystal, which causes a notable delay between the 400 and 800 nm pulses at the output of the crystal in the case of 30fs pulses. Each 0.1 mm of BBO causes ~ 19 fs delay between the driving (800 nm) and second harmonic (400 nm) waves. Thus only a small part of the second harmonic remains within the pulse duration of the driving fundamental 800nm pulse. This causes a further decrease in the influence of the second harmonic field on the whole pattern of harmonic distribution. On the other hand, this second harmonic pulse generates relatively strong low-order odd harmonics: H₅_{400nm} which corresponds to H₁₀_{800nm}, and H₇_{400nm} which corresponds to H₁₄_{800nm}, see Fig. 6. An introduction of either positive or negative chirp in the femtosecond pulses by varying the distance between gratings in the compressor led to an increase of the pulse duration and a better overlap of the two orthogonally polarized pulses in the plasma. However, in that case, a decrease of the intensity of the driving pulse led to a general decrease of the whole harmonic yield.

The peculiarity of the gelatin plasma emission and TCP-induced harmonic spectra was the proximity of some ionic transitions of gelatin with the wavelengths of even harmonics, see H8 and the nearby emission lines of gelatin lines in the case of CdS QD (Fig. 6, middle panel) and ZnS QD (Fig. 6, bottom panel) plasmas. Neither enhancement nor suppression of this harmonic generated in both plasmas was observed. These studies showed that the proximity of strong emission lines and harmonics does not necessarily lead to a variation of the harmonic yield.

We did not make the absolute measurements of harmonic conversion efficiency in QD-containing plasmas. The estimates of conversion efficiency were carried out using the comparison with known results from other plasmas). In the case of silver plasma at similar conditions, we had almost equal conversion efficiencies with regard to ZnS in the range of 40-110 nm. By knowing the conversion efficiency from previous measurements of harmonic generation in the plasmas produced on the surface of bulk Ag (4×10^{-6}), we deduced that

conversion efficiency in ZnS QD plasmas (which was 7 times higher than in bulk ZnS plasma) was $\sim 3 \times 10^{-5}$.

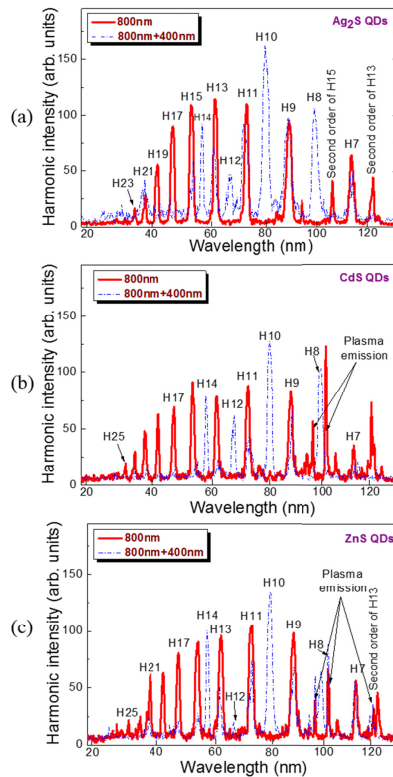


Fig. 6. Two-color (800 nm + 400 nm, dash-dotted blue line) and single-color (800 nm, full red line) pump induced harmonic spectra from Ag₂S (upper panel), CdS (middle panel), and ZnS (bottom panel) QDs at optimal delays between the heating and driving pulses for each species.

4. Discussion

Our experiments have two key features: ablation by nanosecond pulses and QDs-containing targets. So, the observed enhanced HHG conversion efficiency can have three origins: HHG from QDs, HHG from larger concentrations of neutral atoms and HHG enhancement due to the interaction of QDs with atoms. Present studies show that particles with sizes of the order of a few nanometers can effectively generate high-order harmonics. HHG directly from QDs has not yet been studied theoretically, but a simulation of HHG from small clusters [7] showed the increased HHG yield under the assumption of possible recombination of an electron on different atoms in the cluster. The cutoff harmonics were also enhanced much more strongly than the plateau harmonics, which is in good agreement with our experimental results in the case of ZnS QDs (Fig. 4). The local enhancement of the electric field near larger nanoparticles also increases the intensity of cutoff harmonics generated from the surrounding atoms [33].

Early experiments with larger nanostructures [carbon nanotubes, nanoparticles of metals and semiconductors, and other agglomerates of relatively large sizes (20-80 nm)] have shown both merits and drawbacks of this method for increasing the HHG efficiency. An increased recombination cross section of the parent particle with the accelerated electron which, in the case of relatively large particle sizes, may result in an increased number of harmonic emitters is accompanied by a reduced number of atoms located on their surface. In traditional gas HHG, therefore, fewer atoms are involved in the generation of the harmonics because the

atoms located inside the nanoparticles are unlikely to participate in HHG. As a consequence, the amount of harmonic generation processes per single atom falls short for large nanoparticles. Another mechanism for HHG is found in solids [34]. In this case, the electron is excited to a conduction band, and different channels including intraband and interband processes are proposed for the actual generation of the harmonics [35,36]. HHG in solids could also become relevant for nanoparticles. From this perspective, QDs may act as an intermediate material between atoms and solid states. As already mentioned, earlier studies have revealed benefits in using small nanoparticles for HHG [2–13]. The exact number of atoms in the particle for optimal generation of coherent XUV radiation remains a puzzle, despite the fact that, to date, a large number of experiments with gas clusters, as well as ablated nanoparticles, were conducted.

Laser ablation induced HHG spectroscopy of semiconductors can reveal the resonance-induced enhancement of some harmonic orders in the XUV range as well as the cluster-induced growth of harmonic yield. The latter assumption has been demonstrated by de Nalda et al. [16] where the third and fifth harmonic generation of an IR (1064 nm) pulsed laser has been studied in ablation plasmas of the wide bandgap compounds (CdS and ZnS). Their investigation of the temporal behavior of the harmonic generation has revealed the presence of three distinct compositional populations in these plasmas. Species ranging from atoms to nanometer-sized particles have been identified as emitters, and their nonlinear optical properties could be studied separately because they appear at well-separated times in the interaction region with the driving laser pulse. In their experiment, it was found that at earlier times (< 500 ns for the distance chosen for the driving beam) mostly atomic species are responsible for harmonic generation, while clusters mostly contribute at later times (> 1 μ s).

The harmonic generation in such a plasma can prove or disapprove the role of the complex composition of ablated species in this process. A signature which would reveal the nature of the emitters is the growth of harmonics emission with the time delay with respect to the ablation laser pulse. This delay is converted to the time of propagation of QDs or clusters to the interaction region with the ultrashort driving pulse. It was suggested by Oujja et al. [17] that, in the case of a thermalized ablation plume, the average arrival times can be assigned to different cluster sizes. The delay at which the harmonic yield reaches its maximum should scale as a square root of the atomic or molecular weight of the constituents. The ejection of lighter clusters from QDs allows them to reach the region of the driving beam earlier as heavier species.

Therefore QDs comprising of n molecules should appear in the interaction zone $n^{0.5}$ times later compared to single atoms, molecules, or ions of the sulfides. The present HHG studies reveal that for bulk target ablation the maximum yield from single CdS and ZnS molecules occurred at a delay of about ~ 300 – 400 ns. The corresponding QDs allowed efficient generation at about 400–500 ns delay, which is a similar delay as in the former case. Further, attempts to observe HHG at the delays of up to 50 μ s, the expected delay for thermalized larger nanoparticles, did not show any harmonic emission. Thus our studies show that QDs arrive at the area of interaction with the femtosecond laser beam notably earlier than one would expect for a thermalized ablation plume. In other words, all metal sulfide molecules in QDs acquire, from the very beginning, a similar kinetic energy and spread out from the surface with velocities approximately similar to that of single metal sulfide molecule ablating from bulk material. This conclusion reconciles the similarity in the optimal delays for HHG from bulk and QD targets of the same material.

In [16], de Nalda et al. suggested that a similar average kinetic energy $E = mv^2/2$ could characterize all plasma components of the same elemental composition. Thus the average arrival time assigned to the particles containing different amount of identical molecules will be approximately the same. Our studies have confirmed this assumption. The difference in “optimal” delays between heating and driving pulses is related with the difference in the velocities of particles, which depends on the atomic masses of the components of molecules.

One can expect from this assumption the arrival of ZnS ions, atoms and QDs in the area of interaction with driving beam at $(M_{\text{Ag}_2\text{S}}:M_{\text{ZnS}})^{0.5} \sim 1.59$ times earlier with regard to Ag_2S -containing particles taking into account the ratio between the atomic weights of these two molecules ($M_{\text{Ag}_2\text{S}}:M_{\text{ZnS}} \approx 2.54$). Once we compare the “optimal” delays for these two species, their ratio (400 ns: 250 ns = 1.6) becomes close to the above estimates. Thus, one can assume that above rule properly explains the dynamics of material spreading out from the ablated target, once one analyzes the particles’ movement during laser ablation at relatively moderate fluencies ($5 - 20 \text{ J cm}^{-2}$) of heating nanosecond pulses.

As already mentioned, an increase of the recombination cross section for QDs with respect to atoms or single molecules can enhance the HHG efficiency in multi-particle plasmas. An additional cause for strong harmonics generation from QDs compared to single atoms or ions could be the higher concentration of neutral metal sulfide molecules inevitably accompanying the presence of multi-particle species. The QDs present the extreme case of solid-state density in a very small volume. Compared to solids, they still do not absorb all the HHG radiation produced inside them due to their very small thickness. QDs can further improve phase-matching conditions for harmonics generated from atoms and ions [9] using compensation of free-electron dispersion of the driving pulse by dispersion of clusters.

A new method for the analysis of multi-particle plasma formations using two laser sources for the HHG in the laser ablation can be considered as a promising approach to materials science. Its application will expand the possibilities of optimizing HHG in laser-induced plasma plumes, allow the implementation of new approaches to the study of large molecules and clusters undergoing ablation, and will significantly increase the range of objects of study compared to HHG in gases. Thus, the method presented is not only an alternative approach in generating stronger coherent XUV radiation but rather can serve as a tool for various spectroscopic and analytical applications.

5. Conclusions

In this paper, we have studied the possibility and conditions of using quantum dots as efficient emitters for high-order harmonics generation by 30 fs pulses using optimally delayed heating and driving laser pulses.

We further have developed methods for the aqueous synthesis of Ag_2S , ZnS and CdS QDs that enable, by their size and dispersion, as well as their structural properties, the effective generation of harmonics in plasma plumes. The study of the morphological properties of the samples demonstrated the formation of ZnS and CdS QDs with mean sizes of 2-3.2 nm in a cubic lattice, and of Ag_2S QDs with mean sizes of 1.7-2.0 nm in a monoclinic lattice, all with a weight fraction of about 20-25% in gelatin.

A comparison of HHG using QDs and ablation of solid-state targets for the same materials (Ag_2S , ZnS and CdS) was carried out. In the case of QDs, the conversion efficiency into harmonics is higher despite the lower concentration of these species in the plasma compared to the concentration of molecules and ions for bulk ablation. The observed increase of HHG conversion efficiency could be caused by a larger concentration of harmonic emitters and the specific properties of QDs, particularly their plasmonic properties. The maximum HHG conversion efficiency is achieved much earlier than one would expect from the kinetic model of QDs spreading out from the target surface. Therefore similar velocity distributions of molecules and QDs of these metal sulfides are assumed in the ablation process.

Funding

Natural National Science Foundation of China (61774155, 61705227), National Key Research and Development Program of China (2017YFB1104700), Russian Fund for Basic Research (RFBR, 17-52-12034 НННО_а), the German Science Foundation (DFG, Za 110/28-1), Chinese Academy of Sciences President’s International Fellowship Initiative (PIFI, 2018VSA0001).

References

1. C. R. Phipps, *Laser Ablation and Its Applications* (Springer, 2007).
2. T. D. Donnelly, T. Ditmire, K. Neuman, M. D. Perry, and R. W. Falcone, "High-order harmonic generation in atom clusters," *Phys. Rev. Lett.* **76**(14), 2472–2475 (1996).
3. J. W. G. Tisch, T. Ditmire, D. J. Fraser, N. Hay, M. B. Mason, E. Springate, J. P. Marangos, and M. H. R. Hutchinson, "Investigation of high-harmonic generation from xenon atom clusters," *J. Phys. B* **30**(20), L709–L714 (1997).
4. C. Vozzi, M. Nisoli, J.-P. Caumes, G. Sansone, S. Stagira, S. De Silvestri, M. Vecchiocattivi, D. Bassi, M. Pascolini, L. Poletto, P. Villoresi, and G. Tondello, "Cluster effects in high-order harmonics generated by ultrashort light pulses," *Appl. Phys. Lett.* **86**(11), 111121 (2005).
5. S. X. Hu and Z. Z. Xu, "Enhanced harmonic emission from ionized clusters in intense laser pulses," *Appl. Phys. Lett.* **71**(18), 2605–2607 (1997).
6. V. Vénier, R. Taïeb, and A. Maquet, "Atomic clusters submitted to an intense short laser pulse: A density-functional approach," *Phys. Rev. A* **65**(1), 013202 (2001).
7. J. R. Vázquez de Aldana and L. Roso, "High-order harmonic generation in atomic clusters with a two-dimensional model," *J. Opt. Soc. Am. B* **18**(3), 325–330 (2001).
8. T. Tajima, Y. Kishimoto, and M. C. Downer, "Optical properties of cluster plasma," *Phys. Plasmas* **6**(10), 3759–3764 (1999).
9. J. W. G. Tisch, "Phase-matched high-order harmonic generation in an ionized medium using a buffer gas of exploding atomic clusters," *Phys. Rev. A* **62**(4), 041802 (2000).
10. H. Ruf, C. Handschin, R. Cireasa, N. Thiré, A. Ferré, S. Petit, D. Descamps, E. Mével, E. Constant, V. Blanchet, B. Fabre, and Y. Mairesse, "Inhomogeneous high harmonic generation in krypton clusters," *Phys. Rev. Lett.* **110**(8), 083902 (2013).
11. R. A. Ganeev, M. Suzuki, M. Baba, M. Ichihara, and H. Kuroda, "High-order harmonic generation in Ag nanoparticle-containing plasma," *J. Phys. B* **41**(4), 045603 (2008).
12. R. A. Ganeev, M. Suzuki, M. Baba, M. Ichihara, and H. Kuroda, "Low- and high-order nonlinear optical properties of BaTiO₃ and SrTiO₃ nanoparticles," *J. Opt. Soc. Am. B* **25**(3), 325–333 (2008).
13. R. A. Ganeev, P. A. Naik, H. Singhal, J. A. Chakera, M. Kumar, M. P. Joshi, A. K. Srivastava, and P. D. Gupta, "High order harmonic generation in carbon nanotube-containing plasma plumes," *Phys. Rev. A* **83**(1), 013820 (2011).
14. H. Singhal, R. A. Ganeev, P. A. Naik, J. A. Chakera, U. Chakravarty, H. S. Vora, A. K. Srivastava, C. Mukherjee, C. P. Navathe, S. K. Deb, and P. D. Gupta, "High-order harmonic generation in a plasma plume of *in situ* laser-produced silver nanoparticles," *Phys. Rev. A* **82**(4), 043821 (2010).
15. O. Albert, S. Roger, Y. Glinec, J. C. Loulergue, J. Etchepare, C. Boulmer-Leborgne, J. Perrière, and E. Millon, "Time-resolved spectroscopy measurements of a titanium plasma induced by nanosecond and femtosecond lasers," *Appl. Phys., A Mater. Sci. Process.* **76**(3), 319–323 (2003).
16. R. de Nalda, M. López-Arias, M. Sanz, M. Oujja, and M. Castillejo, "Harmonic generation in ablation plasmas of wide bandgap semiconductors," *Phys. Chem. Chem. Phys.* **13**(22), 10755–10761 (2011).
17. M. Oujja, J. G. Izquierdo, L. Bañares, R. de Nalda, and M. Castillejo, "Observation of middle-sized metal clusters in femtosecond laser ablation plasmas through nonlinear optics," *Phys. Chem. Chem. Phys.* **20**(25), 16956–16965 (2018).
18. L. W. Liu, S. Y. Hu, Y. P. Dou, T. H. Liu, J. Q. Lin, and Y. Wang, "Nonlinear optical properties of near-infrared region Ag₂S quantum dots pumped by nanosecond laser pulses," *Beilstein J. Nanotechnol.* **6**(1), 1781–1787 (2015).
19. G. S. Boltaev, B. Sobirov, S. Reyimbaev, H. Sherniyozov, T. Usmanov, M. S. Smirnov, O. V. Ovchinnikov, I. G. Grevtseva, T. S. Kondratenko, H. S. Shihaliev, and R. A. Ganeev, "Nonlinear optical characterization of colloidal solutions containing dye and Ag₂S quantum dot associates," *Appl. Phys., A Mater. Sci. Process.* **122**(12), 999 (2016).
20. P. Kumbhakar, M. Chattopadhyay, and A. K. Mitra, "Nonlinear optical properties of doped ZnS quantum dots," *Int. J. Nanosci.* **10**(1), 177–180 (2011).
21. Z. Zeng, C. S. Garoufalis, A. F. Terzis, and S. Baskoutas, "Linear and nonlinear optical properties of ZnO/ZnS and ZnS/ZnO core shell quantum dots: Effects of shell thickness, impurity, and dielectric environment," *J. Appl. Phys.* **114**(2), 023510 (2013).
22. H. Linnenbank, Y. Grynko, J. Förstner, and S. Linden, "Second harmonic generation spectroscopy on hybrid plasmonic/dielectric nanoantennas," *Light Sci. Appl.* **5**(1), e16013 (2016).
23. R. B. Martin, M. J. Meziani, P. Pathak, J. E. Riggs, D. E. Cook, S. Perera, and Y.-P. Sun, "Optical limiting of silver-containing nanoparticles," *Opt. Mater.* **29**(7), 788–793 (2007).
24. R. Karimzadeh, H. Aleali, and N. Mansour, "Thermal nonlinear refraction properties of Ag₂S semiconductor nanocrystals with its application as a low power optical limiter," *Opt. Commun.* **284**(9), 2370–2375 (2011).
25. O. V. Ovchinnikov, M. S. Smirnov, A. S. Perepelitsa, T. S. Shatskikh, and B. I. Shapiro, "Optical power limiting in ensembles of colloidal Ag₂S quantum dots," *Quantum Electron.* **45**(12), 1143–1150 (2015).
26. C. Hutchison, R. A. Ganeev, T. Witting, F. Frank, W. A. Okell, J. W. G. Tisch, and J. P. Marangos, "Stable generation of high-order harmonics of femtosecond laser radiation from laser produced plasma plumes at 1 kHz pulse repetition rate," *Opt. Lett.* **37**(11), 2064–2066 (2012).

27. C. M. Kim and C. H. Nam, "Selection of an electron path of high-order harmonic generation in a two-colour femtosecond laser field," *J. Phys. B* **39**(16), 3199–3209 (2006).
28. T. Pfeifer, L. Gallmann, M. J. Abel, D. M. Neumark, and S. R. Leone, "Single attosecond pulse generation in the multicycle-driver regime by adding a weak second-harmonic field," *Opt. Lett.* **31**(7), 975–977 (2006).
29. D. Charalambidis, P. Tzallas, E. P. Benis, E. Skantzakis, G. Maravelias, L. A. A. Nikolopoulos, A. Peralta Conde, and G. D. Tsakiris, "Exploring intense attosecond pulses," *New J. Phys.* **10**(2), 025018 (2008).
30. R. A. Ganeev, H. Singhal, P. A. Naik, I. A. Kulagin, P. V. Redkin, J. A. Chakera, M. Tayyab, R. A. Khan, and P. D. Gupta, "Enhancement of high-order harmonic generation using two-color pump in plasma plumes," *Phys. Rev. A* **80**(3), 033845 (2009).
31. R. A. Ganeev, V. V. Strelkov, C. Hutchison, A. Zaïr, D. Kilbane, M. A. Khokhlova, and J. P. Marangos, "Experimental and theoretical studies of two-color pump resonance-induced enhancement of odd and even harmonics from a tin plasma," *Phys. Rev. A* **85**(2), 023832 (2012).
32. I. J. Kim, G. H. Lee, S. B. Park, Y. S. Lee, T. K. Kim, C. H. Nam, T. Mocek, and K. Jakubczak, "Generation of submicrojoule high harmonics using a long gas jet in a two-color laser field," *Appl. Phys. Lett.* **92**(2), 021125 (2008).
33. M. F. Ciappina, S. S. Ćimović, T. Shaaran, J. Biegert, R. Quidant, and M. Lewenstein, "Enhancement of high harmonic generation by confining electron motion in plasmonic nanostructures," *Opt. Express* **20**(24), 26261–26274 (2012).
34. S. Ghimire, A. D. DiChiara, E. Sistrunk, P. Agostini, L. F. DiMauro, and D. A. Reis, "Observation of high-order harmonic generation in a bulk crystal," *Nat. Phys.* **7**(2), 138–141 (2011).
35. O. Schubert, M. Hohenleutner, F. Langer, B. Urbanek, C. Lange, U. Huttner, D. Golde, T. Meier, M. Kira, S. W. Koch, and R. Huber, "Sub-cycle control of terahertz high-harmonic generation by dynamical Bloch oscillations," *Nat. Photonics* **8**(2), 119–123 (2014).
36. G. Vampa, C. R. McDonald, G. Orlando, D. D. Klug, P. B. Corkum, and T. Brabec, "Theoretical analysis of high-harmonic generation in solids," *Phys. Rev. Lett.* **113**(7), 073901 (2014).